TABLE II
FILTER MEASURED PERFORMANCE

	3 μm	1.25 μm
Active Area	1000 mil^2	510 mil^2
Supply Voltage	± 2.5 V	± 2.5 V
Output Swing (RMS) (<1% THD)	3.11 V	3.3 V
Power Dissipation	1250 μW	1250 μW
Clock Frequency	256 Khz	256 Khz
Positive PSRR @ 1Khz	50 dB	50 dB
Negative PSRR @ 1Khz	40 dB	57 dB
Passband Ripple	< ± 0.125 dB	± 0.10 dB
Stop Band Rejection (>4.6Khz)	34 dB	35 dB
THD (4 V_{pp} @ 1Khz)	-67 dB	-69 dB
Dynamic range (C-message wtg)	87 dB	89 dB

tal filters described here. These photos are to scale. Since in the 1.25-μm filter the capacitor array makes up about 60 percent of the filter area, a dramatic further reduction in overall area would require an increase in the capacitance per unit area of the capacitors in the filter so that the capacitance area could be reduced without degrading kT/C noise. Since the dielectric thickness in the capacitors is not set by breakdown field strength considerations but by defect density considerations, there are a number of technological approaches by which the capacitance per unit area could be increased.

REFERENCES

[1] C. K. Wang, "Switched capacitor signal processing circuits in scaled technologies," Ph.D. dissertation, Univ. of California, Berkeley, vol. UCB/ERL M86/84, Nov. 1986.

[2] R. Castello, "Low-voltage low-power MOS switched-capacitor signal-processing techniques," Ph.D. dissertation, Univ. of California, Berkeley, vol. UCB/ERL M84/67, Aug. 1980.

[3] R. Castello and P. R. Gray, "Performance limitations in switched-capacitor filter," *IEEE Trans. Circuits Syst.*, vol. CAS-32, pp. 865–876, Sept. 1985.

[4] R. Castello and P. R. Gray, "A high-performance micropower switched-capacitor filter," *IEEE J. Solid-State Circuits*, vol. SC-20, pp. 1122–1132, Dec. 1985.

[5] C. K. Wang, R. P. Castello, and P. R. Gray, "A scalable high-performance switched capacitor filter," *IEEE J. Solid-State Circuits*, vol. SC-21, pp. 57–64, Feb. 1986.

New Monolithic Switched-Capacitor Differentiators with Good Noise Rejection

CHUNG-YU WU, MEMBER, IEEE, TSAI-CHUNG YU, AND SHIN-SHI CHANG, ASSOCIATE MEMBER, IEEE

***Abstract*—Inverting and noninverting switched-capacitor (SC) differentiators suitable for integrated-circuit implementation are proposed and analyzed. Their structures are simple, parasitic-free, and less sensitive to offset voltage and power-supply voltage changes. In addition, their fabrication process and operating clocks are fully compatible with conventional SC integrators. Noise analysis on the SC differentiators shows a good low-frequency noise-rejection capability. Moreover, the high-frequency noise can be suppressed and does not over-drive the output of the SC differentiators. To demonstrate the application of the SC differentiators in the SC filter (SCF), a bandpass differentiator-type biquad is presented. Both differentiators and biquad were fabricated and measured. The measured differentiation waveforms and the good consistency between the measured and the SWITCAP simulated circuit responses verify the correct operation of the SC differentiators. As a complementary circuit to integrators, the SC differentiators make feasible many interesting new applications and provide different features for the SC circuits.**

Manuscript received December 8, 1987; revised April 25, 1988. This work was supported in part by the National Science Council (NSC), Republic of China, under Grant NSC76-0404-E009-16.

C.-Y. Wu and T.-C Yu are with the Department of Electronics Engineering and the Institute of Electronics, National Chiao Tung University, Hsin-Chu, Taiwan 30039, Republic of China.

S.-S. Chang is with Proton Semiconductor Corporation, Taipei, Taiwan, Republic of China.

IEEE Log Number 8824913.

I. INTRODUCTION

As compared to integrators, little attention has been paid to applying differentiators in analog signal processing systems. The main reason is that circuit performance is severely degraded by high-frequency noise in a classical active-RC differentiator. In many practical systems, however, differentiators are important components for realizing various functions which may not be realizable by integrators. Typical examples are high-pass ladder switched-capacitor filters (SCF's) [1]–[4] and many biomedical, electrochemical, and feedback control systems which require real-time derivative of an analog voltage [5], [6]. Consequently the design of functional differentiators is of considerable interest.

Recently some switched-capacitor (SC) differentiators [2]–[4] were proposed and constructed with discrete elements. Among them, Montecchi [2] proposed a differential bilinear differentiator (BD) which uses a fully differential op amp and three nonoverlapping clocks. Horio and Mori [3], [4] proposed two lossless discrete differentiators (LDD's), which have complex circuit structures.

In this work, new SC differentiators suitable for integrated-circuit realization are proposed. Circuit analysis shows that these new SC differentiators have many advantages and they are fully compatible in fabrication technology and circuit operation with SC integrators [7]. Thermal-noise analysis also shows that high-frequency noise can be suppressed and does not over-drive the circuit. Experimental results on these new SC differentiators and their application circuit are then presented to further confirm the circuit operation and its advantages.

II. INVERTING AND NONINVERTING SC DIFFERENTIATORS

The circuit structure of the proposed inverting differentiator is shown in Fig. 1(a) where ϕ_1 and ϕ_2 are nonoverlapping clocks. Analyzing the circuit operation, it can be shown that the net change of charges on $C1$ during the clock period T is $C1[V_{in}(t_n) - V_{in}(t_{n-1})]$ which also appears on C through induction. The output voltage thus is

$$V_{out}(t_n) = V'_{out}(t_n) = \frac{-C1[V_{in}(t_n) - V_{in}(t_{n-1})]}{C}. \quad (1)$$

Using z transformation, the transfer function $H(z)$ is

$$H(z) = -\frac{V_{out}(z)}{V_{in}(z)} = -\left(\frac{C1}{C}\right)(1 - z^{-1}). \quad (2)$$

Applying the backward-difference (backward-Euler) mapping [8] with $s \leftrightarrow (1 - z^{-1})/T$, (2) becomes

$$H(s) = -s\left(\frac{C1}{C}\right)T. \quad (3)$$

It can be realized from (3) that the SC circuit in Fig. 1(a) performs the differentiation with an equivalent resistor of T/C.

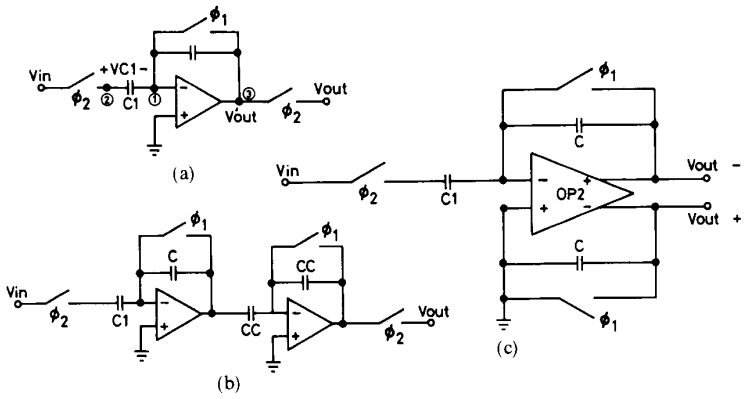

Fig. 1. (a) Circuit structure of inverting SC differentiator. (b) Circuit structure of noninverting SC differentiator with an inverting SC differentiator cascaded by a SC inverter. (c) Merged noninverting and inverting SC differentiators through the use of a fully differential op amp.

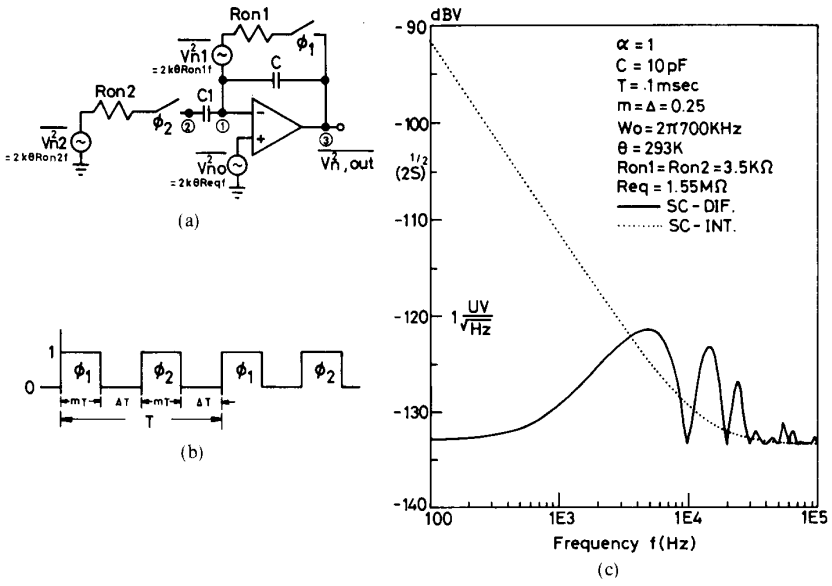

Fig. 2. (a) Noise-equivalent circuit of Fig. 1(a), and (b) the clock waveforms. In $\overline{V_n^2}$ expression, k is the Boltzmann's constant, θ is the absolute temperature, R_{on_i} is the ON resistance of the switch ϕ_i, and R_{eq} is the equivalent input thermal noise resistance of the op amp. (c) Noise spectra of the inverting SC differentiator and integrator.

Like the inverting SC integrator, the time constant of the SC inverting differentiator is $(C1/C)T$ which is proportional to the capacitance ratio and the sampling period. The time constant, therefore, can be precisely controlled in integrated-circuit technology.

In the operation of the SC differentiator shown in Fig. 1(a), node 1 is always virtually grounded and node 2 is periodically connected to V_{in} through the ϕ_2 switch. Thus the operation is insensitive to parasitic capacitances.

Moreover, the ϕ_1 switch periodically makes the output and the input nodes of the op amp short-circuited. Thus the op amp is always kept at the optimal bias point with the maximum gain and symmetry when signals come in. This makes the circuit less insensitive to offset voltages and power-supply voltage changes.

The proposed inverting SC differentiator uses one op amp, two capacitors, two switches, and nonoverlapping clocks. Its structure is simple and the chip area is small. In addition, it is compatible with the conventional SC integrator [7] both in fabrication process and operating clocks.

The noninverting SC differentiators can be implemented by adding a SC inverter to the output of the inverting differentiator, as shown in Fig. 1(b). This structure requires two op amps, four capacitors, and three switches. Another way to implement the noninverting SC differentiator is through the use of a fully differential op amp as shown in Fig. 1(c). In this structure, the inverting output V_{out}^- performs the function of the inverting differentiator. If the same ϕ_1 switch and capacitor C are added to the noninverting output as a dummy load, both outputs have the same loads and the noninverting output V_{out}^+ has a symmetric but opposite output voltage. Thus it acts as a noninverting SC differentiator. Moreover, it can also be used as a fully differential SC differentiator. Both types of noninverting SC differentiators have all the advantages of the inverting differentiator except that the chip area is larger.

III. Noise Analysis

In the frequency domain, the transfer function of (2) can be rewritten as

$$H(e^{jwT}) = -\left(\frac{C1}{C}\right)(1 - e^{-jwT}) \tag{4}$$

where w is the angular frequency. If wT is much smaller than unity, (4) becomes

$$H(e^{jwT}) \simeq -jw\left(\frac{C1}{C}\right)T, \qquad wT \ll 1. \tag{5}$$

Thus, if the signal frequency is much smaller than the sampling frequency, this is an ideal differentiator function with the gain linearly proportional to w. Low-frequency noise, therefore, is not significantly amplified to disturb the signal. But in the high-frequency range, (5) is no longer valid since wT is not much smaller than unity. Thus, unlike the active-RC differentiator, the high-frequency noise in the SC differentiator follows (5) and is not overamplified to saturate the circuit. This feature will be further verified by the following mathematical analysis.

Since only high-frequency noise is of great concern, the following analysis considers the thermal noise rather than the flicker noise. The modeling approach proposed in [9] will be applied to analyze the internally generated thermal noise of the inverting SC differentiator of Fig. 1(a) at output node 3. Since the noninverting SC differentiator is derived from the inverting one, similar noise characteristics are expected.

The thermal-noise equivalent circuit of the SC inverting differentiator is shown in Fig. 2(a) with the clocks given in Fig. 2(b). In the equivalent circuit, all the thermal-noise sources originated from the op amp ($\overline{V_{n0}^2}$) and the incremented channel ON resistance of the MOS switches ($\overline{V_{ni}^2}$) are shown with their mean square voltages $\overline{V_n^2}$ in the frequency range f. Note that only the internally generated thermal noise is to be calculated. Thus the external input noise source and the output ϕ_2 switch are not included in Fig. 2(a) and node 3 is taken as the output node. Later the transmission of the calculated noise to the next stage will be discussed.

The thermal noise internally generated at output node 3 of the inverting SC differentiator is composed of a continuous-time broad-band unsampled noise and a sampled-and-held noise [9]. To calculate the unsampled noise, the three noise sources $\overline{V_{n1}^2}$, $\overline{V_{n2}^2}$, and $\overline{V_{n0}^2}$ are assumed to be uncorrelated so that their contributions can be linearly superposed. For $A_0 \gg 1$, $w/w_0 \ll 1$, and $R_{on2} \ll 1/w_0$ where A_0 is the midband gain and w_0 is the unity-gain frequency of the op amp, the averaged power spectral density (PSD) in the period T at the output is

$$S_d(f) = 2mk\theta\left[\alpha^2 R_{on2} + (1+\alpha)^2 R_{eq} + R_{on1} + \left(\frac{1-m}{m}\right)R_{eq}\right] \tag{6}$$

where α is the capacitance ratio $C1/C$ and m is the duty cycle of the clocks ϕ_1 and ϕ_2 as indicated in Fig. 2(b). In (6), the first two terms are contributed by $\overline{V_{n2}^2}$ and $\overline{V_{n0}^2}$ when $\phi_1 = 0$ and $\phi_2 = 1$. The third term is contributed by $\overline{V_{n1}^2}$ when $\phi_1 = 1$ and $\phi_2 = 0$. The last term is the output noise due to $\overline{V_{n0}^2}$ when $\phi_2 = 0$ and $\phi_1 = 0$ or 1.

The sampled-and-held noise of the SC differentiator is stored on the capacitor $C1$ at the end of the clocks ϕ_2, and then is transferred as a sampled-data signal to the output. Since the sampled-and-held noise stored on $C1$ is further subjected to the operation of the inverting differentiator when transferred to the output, it has to be multiplied by the magnitude of the transfer function $|H(jwT)|$ in (4). The PSD formula for this sampled-and-held noise is the same as its corresponding one in the SC integrator [9] except that $|H(jwT)|$ is different. From [9, eq. (11)], the formula for the SC differentiator is

$$S_{sh}(f) = \frac{T}{2}\Delta^2 \frac{\sin^2\left(\frac{\Delta\pi f}{f_s}\right)}{\left(\frac{\Delta\pi f}{f_s}\right)^2}(R_{on2} + R_{eq})2k\theta w_c \left|2\alpha \sin\left(\frac{\pi f}{f_s}\right)\right|^2 \tag{7}$$

where f_s is the sampling frequency and w_c is the cutoff frequency of the SC differentiator when $\phi_2 = 1$. Assume $R_{on2}C1 \ll 1/\omega_0$, we have $w_c \simeq w_0/(1+\alpha)$ [9].

Substituting w_c into (7) and adding the two types of noises together, the total thermal noise in the inverting SC differentiator can be formulated. Under the same conditions, the noise spectra of both the SC integrator [9] and the SC differentiator are calculated and plotted in Fig. 2(c). As expected, the internal thermal noise of the SC differentiator in the low-frequency range can be more efficiently suppressed than that of the SC integrator. In the high-frequency range, the internal thermal noise does not saturate the SC differentiator.

When $\phi_2 = 1$, the above calculated thermal noise at output node 3 of the SC differentiator is transmitted to the next stage with the signal. So it can be treated as $\overline{V_{n2}^2}$ in the next stage.

IV. Experimental Results

To experimentally verify the operations, the SC differentiators and their application circuits were designed in two testing chips which were fabricated in a 3.5-μm p-well CMOS analog process with poly-n$^+$ capacitors.

The single-ended op amps used in the inverting SC differentiator (Fig. 1(a)) and the noninverting SC differentiator (Fig. 1(b)) are the conventional CMOS two-stage op amp [10]. The fully differential op amp in the noninverting SC differentiator of Fig. 1(c) is a specially designed CMOS fully differential op amp with a high and symmetric driving capability. No common-mode feedback (CMFB) circuit is required in fully differential op amps for this application because one of the two outputs in the op amps is periodically connected to ground whereas the other is periodically connected to the virtual-ground node. This automatically eliminates the common-mode output voltage.

The measured frequency responses of the fabricated inverting and noninverting SC differentiators with $C1 = 1.8$ pF and $C = 0.6$ pF are plotted in Fig. 3(a) where the sampling frequency f_s is 18.85 kHz and the center frequency f_c is 1 kHz. The corresponding SWITCAP [11] simulated result is also shown and is close to the measured results. As expected, the gain is linearly proportional to frequency w if $wT \ll 1$.

To investigate the operation of the fabricated SC differentiators in differentiating an analog voltage, a sawtooth waveform was input and the output voltage was measured. The output waveform is a square wave as shown in Fig. 3(b). It is seen that the differentiator is not saturated or overdriven by high-frequency noise or other input transients.

As an example to demonstrate the application of the developed SC differentiator, a bandpass biquad designed by using the differentiators and fabricated in the test chips is presented here. The circuit structure is shown in Fig. 4(a) where the dummy load for the noninverting SC differentiators is also shown.

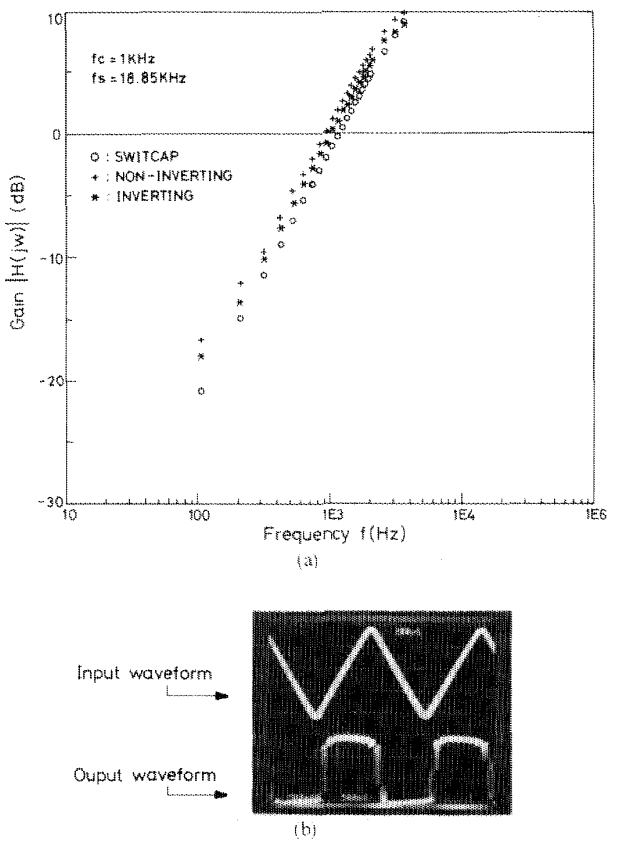

Fig. 3. (a) Measured and simulated frequency responses of the SC differentiators. (b) Measured output waveforms at the noninverting output of Fig. 1(c) with a ramp input.

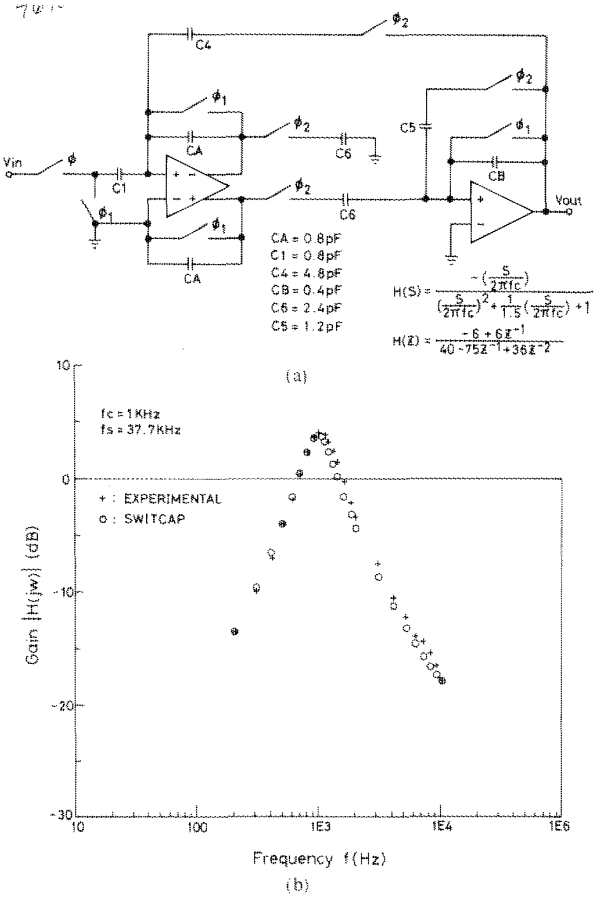

Fig. 4. (a) Circuit diagram of the SC bandpass biquad designed by using noninverting differentiator of Fig. 1(c). (b) Measured and simulated frequency responses of (a).

The implemented s-domain and z-domain transfer function of the biquad is also listed below the circuit diagram. The measured and SWITCAP simulated frequency responses are shown in Fig. 4(b). Good agreement between the measured and the simulated responses confirms the correct operation of the SC differentiators.

V. Summary

Monolithic inverting and noninverting SC differentiators are proposed, analyzed, and experimentally tested. An application circuit is also presented. It is shown that the proposed SC differentiators have simple, concise, and stray-insensitive structures. In addition, they are less sensitive to the offset voltage and the power-supply voltage changes. Noise analysis shows that the SC differentiators have a low internally generated thermal noise in the low-frequency range. Its magnitude is about 40 dBV less than that in conventional SC integrators. Moreover, it is shown that high-frequency noise does not saturate the SC differentiators. Since the proposed SC differentiator is fully compatible in fabrication technology and circuit operation with the SC integrator, it can be conveniently used in a chip to realized SCF's and other analog functions. It can also be used with SC integrators to implement more functions. Thus the design flexibility and the application field of SC circuits can be extended.

Various interesting application circuits of the new SC differentiators, e.g., biquads, ladder filters, FIR filters, etc., have been successfully designed and analyzed. They will be reported on in the near future.

References

[1] E. S. K. Liu, L. E. Turner, and L. T. Bruton, "Exact synthesis of LDI and LDD ladder filters," *IEEE Trans. Circuits Syst.*, vol. CAS-31, pp. 369–381, Apr. 1984.

[2] F. Montecchi, "Bilinear design of high-pass switched-capacitor ladder filters," in *1985 ISCAS Proc.*, pp. 547–550.

[3] Y. Horio and S. Mori, "Switched-capacitor lossless discrete differentiators with modified sample-and-hold sequence," *Electron. Lett.*, vol. 21, pp. 1036–1037, Oct. 1985.

[4] Y. Horio and S. Mori, "SC modified lossless discrete differentiators and resulting SC highpass ladder filters," *Electron. Lett.*, vol. 22, pp. 97–99, Jan. 1986.

[5] J. Nolte, "A differentiator for low-frequency signals," *IEEE Trans. Biomed. Eng.*, vol. BME-25, pp. 554–556, Nov. 1978.

[6] C. Velayudhan and J. H. Bundell, "An improved differentiator for slowly varying signals," *Int. J. Electron.*, vol. 56, pp. 229–234, Feb. 1984.

[7] R. Gregorian and W. Nicholson, "CMOS switched-capacitor filters for a PCM voice CODEC," *IEEE J. Solid State Circuits*, vol. SC-14, no. 6, pp. 970–980, Dec. 1979.

[8] L. R. Rabiner and B. Gold, *Theory and Application of Digital Signal Processing*. Englewood Cliffs, NJ: Prentice-Hall, 1975.

[9] C.-A. Gobet and A. Knob, "Noise analysis of switched capacitor networks," *IEEE Trans. Circuits Syst.*, vol. CAS-30, no. 1, pp. 37–43, Jan. 1983.

[10] P. R. Gray, "Basic MOS operational amplifier design—An overview," in *Analog MOS Integrated Circuits*. New York: IEEE Press, 1980, pp. 28–49.

[11] S. C. Fang, Y. P. Tsividis, and O. Wing, "SWITCAP: A switched-capacitor network analysis program—Part I and part II," *IEEE Circuits Syst.*, pp. 4–10, Sept. 1983, and pp. 41–46, Dec. 1983.